for sucrose[30] and most likely are the explanation for the observed change in the tRNA correlation times (Table V). The ability of the proposed model to account for the change in the relaxation rates upon a change of solvent also demonstrates that intermolecular dipolar relaxation is not contributing to the relaxation of the uridine C-4 carbons in tRNA. The values of η for the uridine lines at this temperature are within experimental error of the theoretical minimum of 0.15 for a body tumbling outside the limit of motional narrowing.[34,35] The decrease in η upon changing to D_2O is an indication of the decrease in the importance of dipolar relaxation in the C-4 uridine carbons. There is no readily apparent explanation for the increase in η for dihydrouridine upon changing to a D_2O solvent. If the true value in both H_2O and D_2O were about 0.5, then one could cite this as evidence, along with the narrow line shape, of the presence of segmental motion in excess of that experienced by the uridines.[35]

A comparison of the calculated τ_R values for the uridines with those of the dihydrouridines at all temperatures shows a 40% lower rate of reorientation for the dihydrouridines. The narrow dihydrouridine line, as pointed out above, and the slightly higher η values for this nucleoside both suggest that the lower than expected relaxation rates for this moiety are due to the presence of a greater amount of segmental motion in the D loop than experienced by the uridines in the rest of the molecule. At 84.6 kG the uridine relaxation rate is seen to decrease by 47%. According to eq 3-6 this change should have been about 80% for a molecule tumbling outside the limit of motional narrowing. This discrepancy, also reflected in Table V, must be more fully documented with more accurate relaxation rate measurements at the higher field before any attempt can be made to reconcile the differences. The significance of the high field relaxation rate measurement, albeit somewhat approximate, is that the results validate the model used to analyze the data.

As the sample temperature is raised from 37 to 45 and then to 60 °C, with the exception of U-3, little change is seen in the uridine relaxation rates and η's. The dihydrouridine relaxation rates and η's generally follow the uridine values up to 45 °C. At 60 °C, however, the dihydrouridine relaxation rate decreases from 0.56 to 0.40 s^{-1} (a 29% decrease) and η goes from 0.2 to 1.0. While the calculated slow τ_R's indicate a 42% increase in the correlation time for this moiety, the increase in η clearly demonstrates that at 60 °C there has been a significant increase in the motional freedom for the dihydrouridines. The dramatic change in the uridine band shape (Figure 5) at 60 °C along with the small but significant decrease in the relaxation rate of the U-3 line and similar increase in its η are further indication that collapse of the tRNA has begun. These data suggest some of the details of melting: that the D and TΨC loops have broken apart and that some of the secondary structure involving base pairs may have been lost. The uridine relaxation rates and η's suggest, however, that considerable secondary structure remains, presumably held together by the base pairs in the stems which are partially holding the molecule together and preventing totally random coil type reorientation from dominating the uridine relaxation rates.

Acknowledgments. This work was presented at the 8th International Conference on Magnetic Resonance in Biological Systems, Nara, Japan, Sept 1978. This work was supported in part by the U.S. Public Health Service through the National Institutes of Health under Awards GM08521 and RR00574. The synthesis of the carbon-13 labeled uracil was supported by ERDA Award E(11-1)-2451. The authors are indebted to the Stanford Magnetic Resonance Laboratory supported by National Science Foundation Award GP23633 and National Institutes of Health Award RR00711 and to Dr. Woody Conover for the 84.5-kG data. One of the authors (W.D.H.) is indebted to the National Science Foundation for support in the form of a Predoctoral Fellowship and to the National Institutes of Health for Postdoctoral Fellowship GM05546. The authors also wish to thank Dr. James McClosky for the mass spectroscopic analysis and Dr. John Ingraham for supplying the *Salmonella typrimurium* JL-1055 culture.

Thermally and Photochemically Initiated Polymerization Processes in the Solid State

Jeremy K. Burdett[1]

Contribution from the Department of Chemistry, The University of Chicago, Chicago, Illinois 60637. *Received February 5, 1980*

Abstract: A simple method, which allows the calculation for solid-state structures of the molecular orbital structure of a fragment within the solid, is described. The resulting orbitals, a subset of the crystal orbitals, allow study of the way an isolated molecular fragment is attached to its solid-state environment. The derivation of correlation diagrams which relate the orbitals of a monomeric unit to those of the same fragment bound into an infinitely repeating polymer allows comment on whether such a polymerization process is thermally or photochemically allowed. For two specific examples, those of $S_2N_2 + \Delta \rightarrow (SN)_x$ and $RC{\equiv}CC{\equiv}CR + h\nu \rightarrow (RCC{\equiv}CC(R){=})_x$, thermally and photochemically allowed processes, respectively, are found.

Introduction

The Woodward-Hoffmann rules[2] and their associated molecular orbital background in terms of orbital symmetry conservation are now well established in organic chemistry. Their use often allows ready prediction of the experimental conditions, thermal or photochemical, for successful generation of desired products. Whether or not polymerization reactions in condensed media are amenable to a similar treatment has not been tackled in an analogous way. This is due, in part at least, to the fact that, whereas the molecular orbitals of the monomeric species are readily derived, the orbitals of the polymeric products are defined in terms of the Bloch functions which take into account the infinite but periodically repeating nature of the "molecule" and are usually represented as the electronic band structure of the solid.[3] In this

(1) Fellow of the Alfred P. Sloan Foundation and Henry and Camille Dreyfus Teacher-Scholar.

(2) Hoffmann, R.; Woodward, R. B. "The Conservation of Orbital Symmetry"; Verlag Chemie: Weinheim/Bergstr., West Germany, 1970.

(3) See, for example, Stiddard, M. B. H. "The Elementary Language of Solid State Physics"; Academic Press: New York, 1975.

0002-7863/80/1502-5458$01.00/0

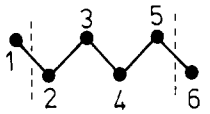

Figure 1. Atoms of an infinite chain showing two repeat units enclosed between dashed lines. The fragment-within-the-solid orbitals are obtained by adding the off-diagonal elements between orbitals on atoms 5 and 6 to the corresponding ones between atoms 2 and 5.

paper we develop a simple method which allows derivation of the molecular orbital levels of the monomeric "fragment within the solid" and allows ready correlation of the orbitals of reactant and product. In this way the orbital correlation principles may be used to comment on whether such processes are thermally or photochemically allowed. We shall describe two examples in detail: that of the thermally induced polymerization of the cyclic S_2N_2 molecule to $(SN)_x$ and the photochemically initiated polymerization of diacetylenes RC≡CC≡CR.

Method

Extraction of a fragment, perhaps one or two repeat units, of the polymer and the derivation of its level structure are clearly not good ways to understand the solid state electronic environment since the "loose ends" of the fragment have low-energy orbitals which are involved in bonding to the rest of the solid. However, we can simulate the energetic behavior of these potent orbitals using an age-old theoretical solid-state device, by imposing cyclic boundary conditions on the orbital structure. With reference to Figure 1 this may be done in a particularly simple way. If we choose as a repeating unit the set of atoms 2–5, then in the solid-state environment atom 2 feels the influence of atom 1 and atom 5 feels the influence of atom 6. Neither atom 1 nor 6 is included in the fragment we have chosen. However, we may readily calculate the orbital overlap integrals between these atom pairs and the corresponding off-diagonal elements of the secular determinant of a molecular-orbital calculation. Addition of the off-diagonal terms between atoms 5 and 6 to those between 2 and 5 (small because of the large distance between them) and completion of the molecular orbital calculation lead to the orbitals of the "fragment within the solid". Atom 2 feels an interaction of just the right magnitude expected from atom 1 and atom 5 feels a similar interaction with atom 6. What we have done is tie the ends of the fragment together in Hilbert space.[4] As an example we derive the "fragment within the solid" orbitals for simple linear polyenes (**1**–**4**). In a recent paper[5] Whangbo, Hoffmann, and

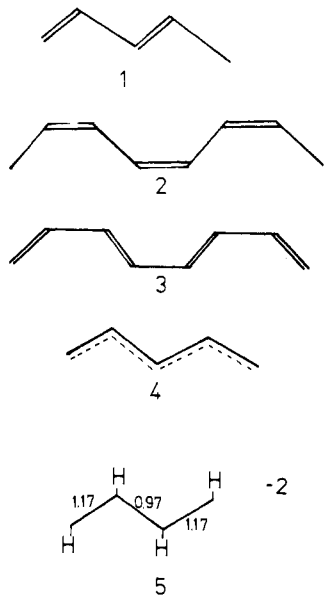

Table I. Energies of Polyene Isomers

geometry	energy[a] (this work)	energy[a,b] (band structure)
1	0.0	0.0
2	41[c]	9.6
3	36.2[c]	10.9
4	7.82	1.8

[a] Relative to **1**. Energies per C_4H_4 unit, kcal/mol. [b] From ref 5. [c] We note rather higher energy differences between **2**, **3** and **1**, **4** using the present method. These large energy differences between isomers compared to the WHW results are not found for other systems we have studied, e.g., the polyphenylenes. The stability of **1**, **4** over **2**, **3** lies within the σ framework and is probably due in part to close H···H repulsions in the latter.

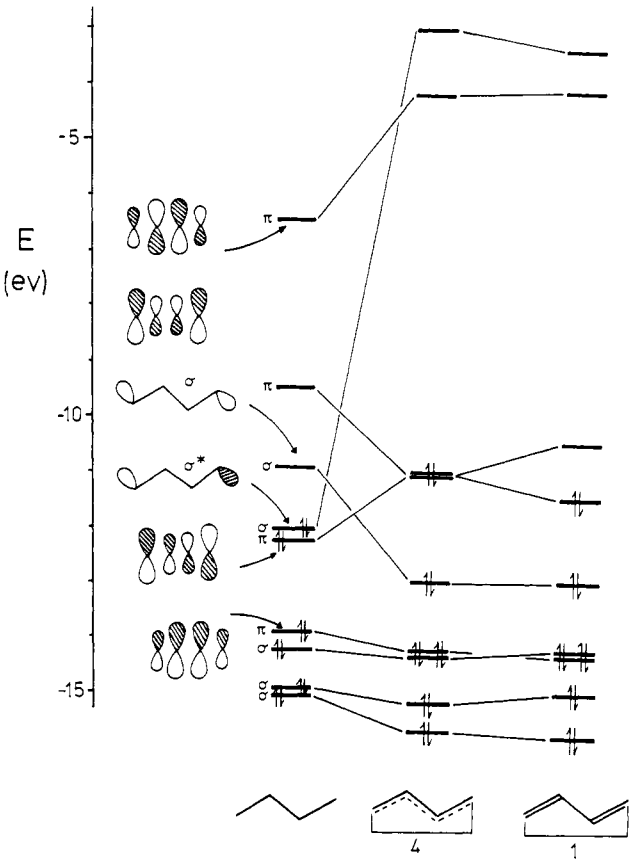

Figure 2. Generation of the fragment-within-the-solid orbitals of **1** and **4**. The thinner line shown joining the ends of these units in the figure denotes a calculation where the ends of the fragments have been tied together. Since two repeat units have been used the orbitals are the subset of the crystal orbitals at $\mathbf{k} = 0$ and at the zone edge.

Woodward (WHW) have calculated the band structures of these systems, using the extended Hückel method.[6] Here we use the same method to derive our molecular orbital energy diagrams. The parameters are given in the Appendix and some numerical results of interest are given in Table I.

Both types of calculation clearly put the cis isomers **2** and **3** at highest energy and the trans isomers **1** and **4** at lowest energy. They both agree that **1** is most stable but disagree as to which of the unfavorable cis isomers is of lower energy. Similar values for the electronic energy per $(CH)_2$ fragment are found if we choose just one repeat unit of the solid (two carbon atoms for **1** and **4**) or two repeat units (four carbon atoms for **2** and **3**).

Figure 2 shows the derivation of the molecular orbital diagram of **4** within the polymer from that of the C_4H_4 fragment of the

(4) The method is not new and has its origins buried in the solid-state literature. Perhaps the best discussion of the approach is given by Zunger, A *J. Phys. C* **1974**, *7*, 76. *J. Chem. Phys.*, **1975**, *62*, 1861; **1975**, *63*, 1713.

(5) Whangbo, M-H; Hoffmann, R.; Woodward, R. B. *Proc. R. Soc. London, Ser. A* **1979**, *366*, 23.

(6) Hoffmann, R. *J. Chem. Phys.* **1963**, *39*, 1397. Hoffmann, R.; Lipscomb, W. N. *Ibid.* **1962**, *36*, 3489; **1962**, *37*, 2872.

same geometry, and its distortion to the lower energy form **1**. With the aid of the atomic orbital composition of the orbitals of the isolated C_4H_4 fragment before its ends are tied together, the generation of the diagram for **4** is simple. The only orbitals which change in energy significantly when the ends of the unit are tied together are those with sizable coefficients of orbitals located on the end atoms which point in the correct direction to interact with the next atom in the chain. If the coefficients of these frontier orbitals at each end of the chain are in phase, then a stabilization results; if they are of opposite sign, a destabilization results. Figure 2 clearly shows a σ bonding and σ antibonding interaction associated with the orbitals labeled σ and σ^*. These are the orbitals responsible for linking the unit of 4 to its surroundings in the polymer. They cross over in energy on moving from the isolated fragment to the polymer orbitals. Thus the nature of the HOMO is different in the isolated fragment and in the fragment within the solid.

The behavior of the π orbitals is rather different. All four π orbitals of the fragment change in energy on moving to the polymer; the highest energy orbital is destabilized and the lowest energy orbital is stabilized. The middle two orbitals of the fragment become degenerate in the polymer structure. Thus, although a σ bond is formed when the unit is placed in the polymer, the occupied π-type orbitals overall receive a destabilization. The π-orbital structure of this unit is readily seen to be isomorphous to that of cyclobutadiene. Here then is an explanation for the distortion of **4** to the experimentally observed structure **1**. Just as this small organic molecule in its lowest singlet state is predicted to distort away from the D_{4h} geometry to relieve the asymmetric occupation of degenerate orbitals via a pseudo-Jahn–Teller process, so the regular linear polymer is predicted to distort to a structure containing alternating single and double bonds. This is the Peierls' distortion[7] in one-dimensional systems at its simplest. The degeneracy is clearly imposed in our model by the translational symmetry of the system. Interestingly, with two extra electrons per fragment ($(NH)_n$ or S_n) the symmetric structure **4** is predicted to be most stable just as $C_4H_4^{2-}$ is predicted to be square planar and actually found in this geometry in, for example, $Fe(CO)_3(C_4H_4)$, formally written as $Fe^{II}(CO)_3(C_4H_4)^{2-}$. This nonalternating bond arrangement is found experimentally in the structures of fibrous sulfur and of elemental selenium and tellurium.[8]

The occupied orbitals of the isolated fragment do then differ in nature from the fragment within the solid as was to be expected. We noted above that within the σ manifold two orbitals crossed over in energy on tying together the ends of the unit. Use of the molecular orbitals of the isolated fragment to describe the polymeric material is then not a good one. Such a method, however, is often used to calculate Madelung potentials and relaxation energies in X-ray PES studies[9] (molecular cluster calculations). Usually in such cases the "loose ends" are saturated with electrons before the comparison between the cluster and extended solid is made. **5** shows the population analysis for such a $C_4H_4^{2-}$ unit

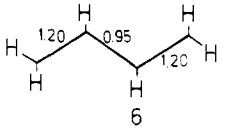

6

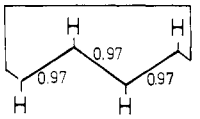

7

where the ends have not been tied together. Even though all CC bond lengths were put equal in the calculation, the bond overlap populations alternate along the chain.[10] A similar result occurs (**6**) if the ends of the unit are saturated with hydrogen atoms, a popular way[11] of simulating the environment in silicate and other tetrahedrally coordinated structures. Equal bond overlap populations are found (**7**) by using the present method since both the σ- and π-bonding requirements of the terminal atoms are satisfied.

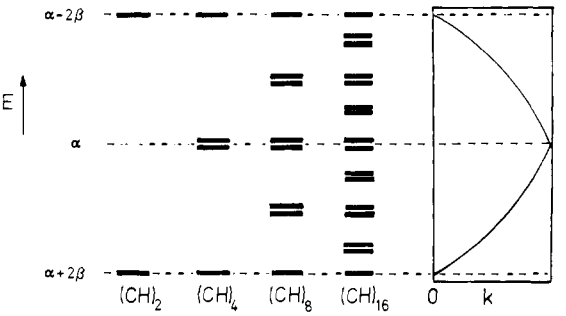

Figure 3. The meaning of the fragment-within-the-solid orbitals. π orbital structure for a number of different $(CH)_n$ fragments when their ends are tied together. At the far right is shown the π band structure.

What then do the orbitals of the fragment within the solid actually represent? For the π manifold of the polyene chain the connection between these orbitals and the band structure of the infinite solid is easy to see. As we will show, our present method of calculation produces a subset of the crystal orbitals and may be regarded as an approximation to a band structure calculation. With reference to Figure 3 the π orbitals of the C_4H_4 unit of **4** before its ends are tied together are those of butadiene with orbital energies according to simple Hückel theory of $\epsilon = \alpha \pm \beta(\sqrt{5} \pm 1)/2$. As the length of the chain increases, then the energy of the highest π orbital approaches $\epsilon = \alpha - 2\beta$ and that of the lowest lying π orbital approaches $\epsilon = \alpha + 2\beta$. (The general equation for the jth level energy of an n-membered chain is $\epsilon_j = \alpha - 2\beta \cos(j\pi/(n+1))$.) In between lie a collection of other orbitals. The band structure calculation for the infinite solid shows[5] two π bands, the lower stretching in energy from $\alpha + 2\beta$ to α and the other from α to $\alpha - 2\beta$. The molecular-orbital structure of the "fragment within the solid" by applying the cyclic boundary conditions defines in this case the energies of the top and bottom of the two π bands of the polmer. In general, depending on fragment choice they will represent a particular subset of the crystal orbitals. Selection of just the repeat unit itself leads to the band structure at $\mathbf{k} = 0$; two fragments will give the orbital energies at the zone boundaries and larger fragments give orbital energies which fall between the two. Messmer and co-workers have employed[12] a very similar method to view the chemisorption process occurring on sheets of atoms in a graphite-like array by considering an 18-atom raft with its ends, now in two dimensions, tied together. Their conclusion concerning the validity of the approach was that for reasonably smooth energy bands (in $\mathbf{k}$ space) a rather small error was introduced by such a replacement. The numerical advantage of the technique is that the presence of a finite rather than an infinite collection of atoms means that the total energy of the system may be obtained by a finite summation over all occupied orbitals rather than by an integration over $\mathbf{k}$ space. Conceptually the use of rather a small number of atoms means that the reasons for energy changes on distortion, namely, how the overlap integrals change as the molecule is deformed, are

(7) Peierls, R. E. "Quantum Theory of Solids"; Oxford University Press: London, 1955.
(8) Although the atoms in these species are arranged in spirals rather than lying in the same plane.
(9) For example, Tossell, J. A.; Gibbs, G. V. *Phys. Chem. Miner.* **1977**, *2*, 21.
(10) To date molecular cluster calculations have been performed on systems containing atoms of disparate electronegativity. For example, the SiO_4^{4-} unit is used[9] to model the tetrahedral environment of Si in silica (SiO_2). In these cases the extra electrons will be associated with orbitals which are largely oxygen (the more electronegative element) in character and, since this is where they most likely lie in the solid-state structure itself, perhaps the error involved in the molecular cluster calculation is not too large.
(11) See, for example, Louisnathan, S. J.; Hill, R. J.; Gibbs, G. V. *Phys. Chem. Miner.* **1977**, *1*, 53. Tossell, J. A.; Gibbs, G. V. *Am. Mineral.* **1976**, *61*, 287.
(12) Bennett, A. J.; McCarroll, B.; Messmer, R. P. *Phys. Rev. B* **1971**, *3*, 1397.

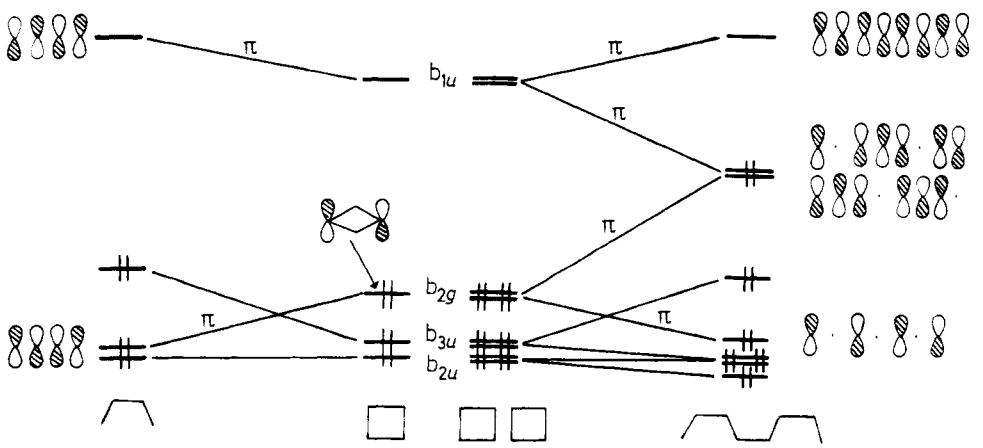

Figure 4. Correlation of the orbitals of S_2N_2 with polymeric $(SN)_x$. At the left is shown the correlation with a single cyclic S_2N_2 molecule. This leads to fragment-within-the-solid orbitals corresponding to $\mathbf{k} = 0$. With two S_2N_2 units the fragment-within-the-solid orbitals are those at the zone edge in addition to those at $\mathbf{k} = 0$. (The b_{2g} of the cyclic system contains p-orbital contributions from the sulfur atoms only.) For simplicity the coefficients of the π orbitals are shown with equal weight.

Table II. Energies of $(SN)_x$ Isomers

geometry	energy[a] (this work)	energy[a,b] (band structure)
9	0	0
10	2.03	0.1
11	19.4	18.3

[a] Relative to the experimental geometry of 9. Energies per S_2N_2 unit, kcal/mol. [b] From ref 5.

readily extracted from the calculation.

Polymerization of Cyclic S_2N_2

One system related to the one-dimensional carbon-based polymers above is $(SN)_x$ polymer[13] obtained by allowing monomeric S_2N_2 (made by pyrolysis of S_4N_4 over silver wire at 200 °C) to polymerize at 0 °C (**8**). An interesting experimental

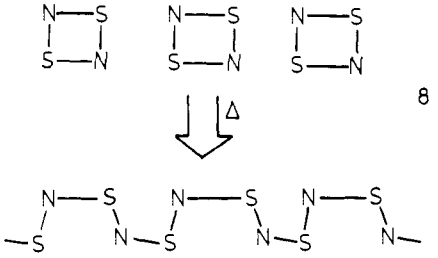

8

observation is that this is an example of a topotactic reaction where the spatial orientations of reactant and product in the solid are closely related. This system contains one more electron (per SN unit) than the polyenes described above, $(CH)_n$. In the selection of a suitable fragment of the solid for calculation we must not forget that the solid-state structure may have extra elements of symmetry not possessed by the simplest repeat unit itself. In the present system structures **9** and **10** have a twofold screw axis which

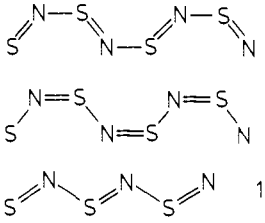

9

10

11

requires in the band structure that the π bands touch at the zone edge. This property has an important bearing on the electrical properties of the polymer. Since the lower energy of these two bands only is occupied, in the absence of a Peierls distortion to remove this degeneracy the system should be (and in fact is) a metallic conductor.[13,14] In our molecular-orbital calculations we need to perform a calculation on a unit large enough to reflect this property, in this case a calculation on the eight-atom fragment S_4N_4. A calculation for such a fragment within the solid shows, in agreement with band-structure calculations,[4] that the cis isomer (**9**) of $(SN)_x$ is of lower energy than the other possible cis form (**10**) and trans form (**11**) (Table II). Only the cis isomer has been made experimentally. It is very interesting to see, however, using our molecular orbital boundary conditions, how the orbitals of two cyclic S_2N_2 monomers before reaction correlate with those of the S_4N_4 unit within the polymer after reaction. In addition we may also view the analogous process starting from a single S_2N_2 monomer. Figure 4 shows the result of a calculation where the geometry of the four-atom unit and its neighbors is gradually changed from the monomeric to polymeric arrangement. The orbitals of the monomer are similar to those found via an SCF Xα calculation.[15] As may readily be seen on polymerization, the occupied orbitals of the monomer very smoothly correlate with the occupied orbitals of the polymer, implying that the reaction is thermally allowed, in accord with the experimental observations noted above. No low-energy occupied monomer orbitals correlate with high-energy empty polymer orbitals. As the polymerization process continues, these fragment-within-the-solid orbitals correlate in a similar fashion with the overall band structure of the solid. Thus the process is clearly thermally allowed. Of the two highest occupied molecular orbitals of S_2N_2 one is of σ and the other of π type. The σ orbital is a lone-pair orbital made up of sp-hybridized functions on the sulfur atoms and virtually pure p orbitals on the nitrogen atoms. As the monomer distorts to the polymeric geometry the directions in which these lone-pair orbitals point change to accommodate the new configuration around the atoms (**12**). The degeneracy of the HOMO for the fragment-within-

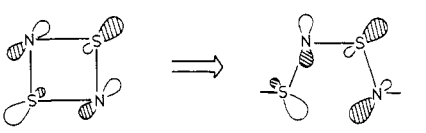

12

the-solid orbitals of S_4N_4 is clear to see in Figure 4. Since one of the unoccupied orbitals of the monomer correlates with one of these degenerate components, then the reaction could also be photochemically allowed.

(13) See, for example, Cohen, M. J.; Garito, A. F.; Heeger, A. J.; MacDiarmid, A. G.; Mikulski, C. M.; Saran, M. S.; Kleppinger, J. *J. Am. Chem. Soc.* **1976**, *98*, 3844.

(14) Kamimura, H.; Glazer, A. M.; Grant, A. J.; Natsume, Y.; Schreiber, M.; Yoffe, A. D. *J. Phys. C* **1975**, *9*, 29.

(15) Salahub, D. R.; Messmer, R. P. *Phys. Rev. B* **1976**, *14*, 2599.

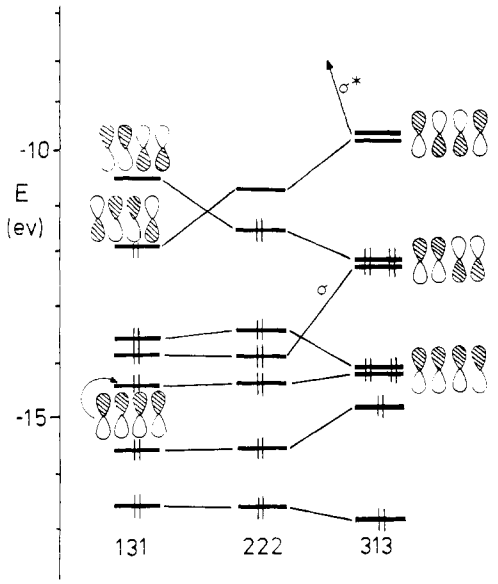

Figure 5. Correlation of the orbitals of the 313 monomer with those of the 131 and 222 polymeric fragments within the solid for diacetylenes, RCCCCR. Calculations were performed for R = H. Only one component of the degenerate π orbitals of the monomer is shown.

Table III. Energies of Polydiacetylene Isomers

geometry	energy[a] (this work)	energy[a,b] (band structure)
14	0	0
15	16.6	11

[a] Relative to 14. Energies per C_4H_2 unit, kcal/mol. [b] From ref 5.

Polymerization of Diacetylenes RC≡CC≡CR

In the solid state, diacetylenes may be polymerized[16] by UV irradiation (**13**). The observed product is the "131" form (**14**)

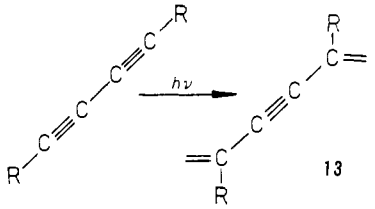

and not the alternative "222" form (**15**). Firstly we look at the

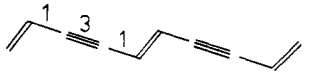

14

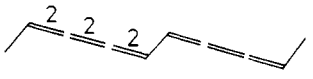

15

orbital structure of these two possible products which have also been the subject of band-structure calculations by WHW.[5] We use in this case a single repeat unit of the polymeric structure in our calculation. Figure 5 shows the fragment-within-the-solid orbitals of the 131 fragment. The derivation of this diagram from that of the isolated fragment is simply obtained by noting the relative phases of the orbitals of the isolated fragment as shown earlier in this paper. On distortion to the 222 structure the HOMO and LUMO exchange roles (Figure 5). The HOMO, however, is stabilized more in the 131 structure than in the 222 arrangement and overall the triply bonded configuration is calculated to be more stable (Table III). Analogous results are found in the WHW band structure calculations.[5] Here the top of the valence band of the 131 structure and the bottom of the conduction band cross over in energy as the structure is distorted to the 222 arrangement.

Table IV. Parameters Used in the Extended Hückel Calculations

atom	orbital	exponent	H_{ii}
H	1s	1.3	-13.6
C	2s	1.625	-21.4
	2p	1.625	-11.4
N	2s	1.950	-26.0
	2p	1.950	-13.4
S	3s	1.817	-20.0
	3p	1.817	-13.3

Of interest to us here is how the orbitals of the monomeric C_4H_2 fragment (a 313 structure) correlate with the orbitals of the 131 polymeric product, also shown in Figure 5. The HOMO and LUMO in the monomer are doubly degenerate and are π-type orbital combinations involving all four carbon atoms. On polymerization the CCH angle closes down from 180 to around 120° and this degeneracy is lost. One component of each of these degenerate pairs is involved in σ bonding to the adjacent unit in the polymer chain. The component derived from the HOMO correlates with a σ bonding orbital and drops in energy, while the energetic behavior of the LUMO-derived component, which correlates with a σ^* orbital, is just the opposite. The remaining components of the HOMO and LUMO become π-type orbitals in the product. In contrast to the S_2N_2 example above, the occupied monomer orbitals do not all correlate with the occupied orbitals of the product. One component of the LUMO of the monomer does, however, correlate with the HOMO of the product and the orbital correlation diagram has all the features associated with a thermally forbidden but photochemically allowed process. As we proceed from the orbitals of the fragment within the solid to the band structure result we find from WHW that the top of the valence band corresponds to an orbital with the same phase relationships between the orbitals of adjacent atoms as the HOMO of the fragment within the solid. Analogously the bottom of the conduction band corresponds to the phasing arrangement found for the LUMO of the fragment within the solid. Thus the orbital structure found for the latter is correctly carried over into the infinite system.

Interestingly, the occupied orbitals of the monomer do correlate with the occupied orbitals of the unstable 222 isomer, which itself is related to the stable 131 form by a thermally forbidden pathway. An orbital diagram showing how the monomer and the two possible products are related is shown in **16**.

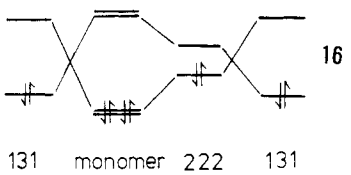

It is interesting to note that our approach in this paper is different from the usual way of viewing such processes in terms of initiation, polymerization, and termination. Whatever the details of these steps, the overall process will be determined by the orbital ideas we have described.

Acknowledgments. Some of the initial work on this problem was tackled by Guy L. Rosenthal. Acknowledgment is made to the donors of the Petroleum Research Fund, administered by the American Chemical Society, for support of this research.

Appendix

The orbital parameters used in the extended Hückel calculations are shown in Table IV. Standard C—C, C=C, C≡C, and C—H bond lengths were used throughout.[17] S=N and S—N distances used were 1.593 and 1.628 Å, respectively. The observed geometries of both S_2N_2 and $(SN)_x$ polymer were used as the end points of the calculations of Figure 4.

(16) For a recent review of solid-state photochemical polymerizations see: Cohen, M. D. *Angew. Chem., Int. Ed. Engl.* **1975**, *14*, 386.

(17) Pople, J. A.; Gordon, M. *J. Am. Chem. Soc.* **1967**, *89*, 4253.